Observation in the Kamiokande-II detector of the neutrino burst from supernova SN1987A

K. S. Hirata and T. Kajita
International Center for Elementary Particle Physics, University of Tokyo, Tokyo 113, Japan

M. Koshiba
International Center for Elementary Particle Physics and Department of Physics, University of Tokyo, Tokyo 113, Japan

M. Nakahata and Y. Oyama
Department of Physics, University of Tokyo, Tokyo 113, Japan

N. Sato
Department of Astronomy, University of Tokyo, Tokyo 113, Japan

A. Suzuki and M. Takita
Department of Physics, University of Tokyo, Tokyo 113, Japan

Y. Totsuka
International Center for Elementary Particle Physics and Department of Astronomy, University of Tokyo, Tokyo 113, Japan

T. Kifune and T. Suda
Institute for Cosmic Ray Research, University of Tokyo, Tokyo 118, Japan

K. Takahashi and T. Tanimori
KEK, National Laboratory for High Energy Physics, Ibaraki 305, Japan

K. Miyano and M. Yamada
Department of Physics, University of Niigata, Niigata 950-21, Japan

E. W. Beier, L. R. Feldscher, W. Frati, S. B. Kim, A. K. Mann, F. M. Newcomer,
R. Van Berg, and W. Zhang
Department of Physics, University of Pennsylvania, Philadelphia, Pennsylvania 19104

B. G. Cortez*
California Institute of Technology, Pasadena, California 91125
(Received 26 February 1988)

The properties of the Kamiokande-II detector and the method of measurement are described in detail. The data on the neutrino burst from the supernova SN1987A on 23 February 1987 at 7:35:35 UT$\pm$1 min are presented, with records of earlier and later observation periods in which other neutrino events possibly associated with SN1987A might have occurred. There is no evidence in the data for any excess of neutrino-induced events, either in a burst of a few seconds duration or over a longer time interval, relative to the usual count rate, excepting only the neutrino burst at 7:35:35 UT. The nature of the single, observed neutrino burst coincides remarkably well with the elements of the current model of type-II supernovae and neutron-star formation. This is the first direct observation in neutrino astronomy.

I. INTRODUCTION

Supernovae, which follow the demise of certain stars when their nuclear fuel is exhausted, have been the subject of speculation for many centuries, and recently, of experimental study and theoretical modeling.[1] Within the last 25 years, two principal types of supernovae have been delineated.[2] Briefly, supernovae of type I seem to follow from the accretion of mass by an aged star of relatively low initial mass, which then, exceeding the Chandrasekar limit,[3] ultimately becomes unstable and explodes, leaving behind only debris. Supernovae of type II are thought to involve stars of mass greater than about eight solar masses wherein the central core of roughly 1.5 solar mass, having carried out nuclear fussion to the point of diminishing return, can no longer resist the pressure exerted by its internal gravitational force, and collapses to a neutron star of small dimension, perhaps 10 km in radius, and nuclear density (10^{17} kg/m^3). By various mechanisms the remainder of the star is excited and radiates energy over much of the electromagnetic spectrum.

Soon after the distinction was made between type-I and type-II supernovae, it was recognized that the release of the binding energy of the neutron star, amounting to 0.1–0.2 solar mass, or approximately 10^{53} ergs, would not take place by the emission of photons, but would be possible through the emission of neutrinos.[4] Neutrinos would be created in the formation of the neutron star via the reaction $e^- + p \rightarrow \nu_e + n$, and, subsequently, in greater abundance in the rapid cooling down of the neutron star from an initial temperature kT in the vicinity of 3–5 MeV. On the basis of quantitative modeling,[5] it had been expected that the average neutrino energy would be in the vicinity of 15 MeV which, for a total emitted energy of $\sim 3\times10^{53}$ ergs, indicated a total neutrino yield of 10^{57}–10^{58} neutrinos. Furthermore, neutrino emission would occur in a time interval of at most a few seconds.

This plausible description of type-II supernovae has been in place without confirmation of its basic elements for roughly two decades. In this paper we describe the direct observation on 23 February 1987 at 7:35:35 UT$\pm$1 min of a burst of neutrinos[6] in a massive, imaging water Cherenkov detector, known as Kamiokande-II, located in a deep mine near Kamioka, Japan. The number of neutrino interactions observed, their characteristics, and the time interval in which the burst occurred are all in excellent agreement with the general aspects of the current model of type-II supernovae mentioned above. The neutrino burst specifies the time of the core collapse of the blue supergiant star Sanduleak $-69°$ 202 in the Large Magellanic Cloud[7] (LMC), now identified as the progenitor of SN1987A, which was first sighted optically[8] about 3 h after the core collapse. The Earth-LMC distance is approximately 55 kpc.

The observation in Kamiokande-II of the neutrino burst from Sanduleak $-69°$ 202 constitutes direct observation in real time of neutrinos from a stellar body outside the Galaxy, and direct evidence of the mechanism of neutron-star formation. A search in the data of another massive, imaging water Cherenkov detector, the Irvine-Michigan-Brookhaven (IMB) detector, located in a salt mine near Cleveland, Ohio, yielded a similar neutrino burst on 23 February 1987 at 7:35:40 UT (Ref. 9), thus directly confirming the Kamiokande-II observation.

In Sec. II of this paper we describe in detail the properties and method of measurement of the detector Kamiokande-II in which the neutrino burst was observed. The neutrino burst data are presented in Sec. III, with records of earlier and later observation periods in which other neutrino events possibly associated with SN1987A might have occurred. Data analysis and interpretation are given in Sec. IV, and a summary and conclusions in Sec. V.

II. THE KAMIOKANDE-II DETECTOR

A. Mechanics and electronics

The Kamiokande-II water Cherenkov detector is located in the Kamioka mine in Gifu prefecture in the region of the Japan Alps. Access to the detector is by a 2800-m adit, at which point the shielding overhead amounts to minimum of 2400 mWe (meters of water equivalent).

A schematic view of the detector is shown in Fig. 1. A detailed description of the original detector is given in the theses listed in Ref. 10. In the upgraded Kamiokande-II detector, 948 photomultiplier tubes (PMT's), each 0.5 m in diameter, are uniformly placed facing inward on a 1-m grid on the entire surface with dimensions 14.4 m in diameter by 13.1 m high, which contains 2140 metric tons of water. The total photocathode surface area of all PMT's is approximately 20% of the total surface area of the 2140-ton fiducial volume. Each PMT is shielded against magnetic fields, and the tank is surrounded by coils in which currents are passed to cancel out the measured Earth's magnetic field. An elaborate water purification system ensures that the attenuation length of the tank water for Cherenkov radiation (300–500-nm wavelength) exceeds 50 m at any time. The attenuation length is regularly monitored by means of cosmic-ray muons passing through the detector. In addition since September 1986 ion-exchange columns have maintained the uranium and radium content in the tank water at less than 10^{-3} pCi/liter, corresponding to less than 10^{-2} Hz in trigger rate. A 4π solid-angle anticounter, also a water Cherenkov counter with 123 PMT's of 0.5 m diameter, surrounds the inner detector. The mean thickness of the water in the anticounter is 1.5 m, and is useful as shielding against gamma rays and neutrons entering the detector as well as for its veto function.

The electronics system provides multihit time and charge measurement capacity for each PMT. The block diagram of the system is shown in Fig. 2. The system records any signal larger than 0.35 photoelectrons (PE's) in a given PMT when an event trigger is present. The

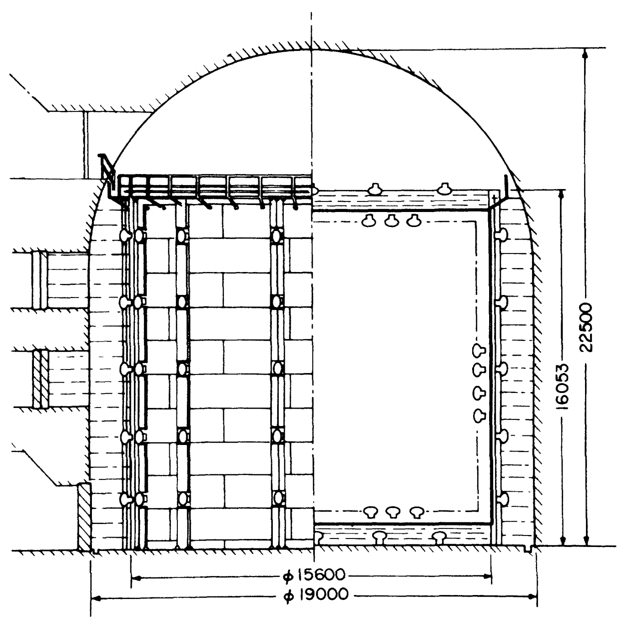

FIG. 1. Schematic outline of the detector, Kamiokande-II. The anticounter is shown by the dashed area. Dimensions are in mm.

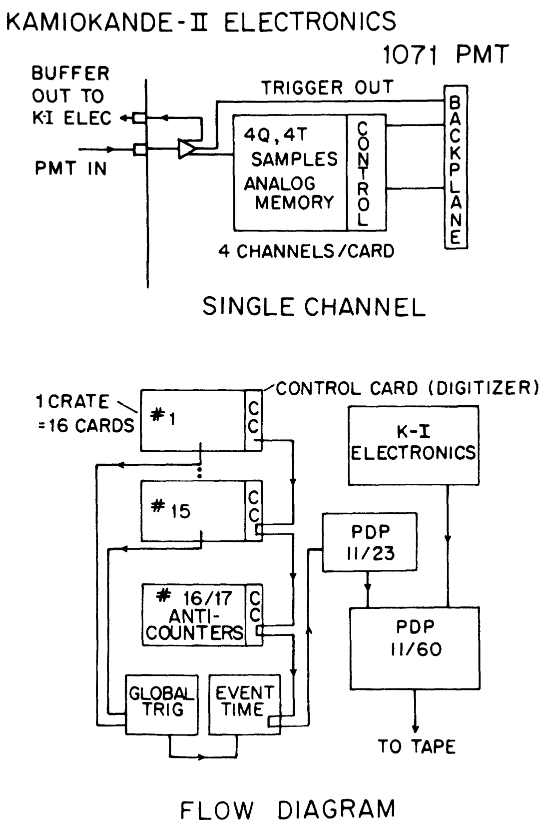

FIG. 2. Block diagram of the Kamiokande-II electronics.

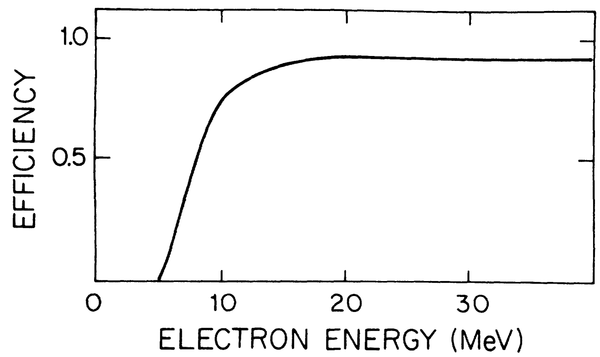

FIG. 3. Trigger efficiency vs electron energy for the 2140-ton fiducial volume. There are 948 PMT's in the central detector and 123 PMT's in the surrounding anticounter.

hardware (global) trigger is formed when 17±2 PMT signals are present within a 100-nsec interval, the spread arising primarily from the time dispersion of the individual PMT signals. The software event trigger is formed by requiring 20 or more PMT signals within 100 nsec, corresponding to 7.5-MeV energy for electrons and positrons, and the trigger deadtime is less than 50 nsec. The trigger efficiency dependence on energy is shown in Fig. 3. The timing information is vital for reconstruction of the vertex position of low-energy electrons. The Monte Carlo-calculated 1σ error on each of the x, y, and z coordinates of the reconstructed vertex position of 10-MeV electrons is 1.0 m. The Monte Carlo model of the detector also yields the energy and angular-resolutions for 10-MeV electrons as mean uncertainties of 22% and 28°, respectively.

B. Energy measurement and calibration

Single low-energy electrons and positrons produced by neutrinos and antineutrinos incident on the detector cause the emission of Cherenkov light with a total intensity nearly proportional to the energy of the charged particle. In the energy regime of the events discussed here, a typical PMT response corresponds to the detection of one photoelectron. Thus, the energy of the charged particle may be estimated by an appropriate sum of the number of PMT's which respond to the signal.

The actual response of the detector to the Cherenkov light depends on attenuation of the Cherenkov light by absorption in the water, Rayleigh scattering in the water, and reflection from the side of the detector, as well as the variation in response of individual PMT, and geometrical effects arising from event location and the location of the responding PMT's. A description of the energy determination for low-energy electrons and positrons, and of the absolute calibration of the energy scale with an uncertainty of less than 5% are given in Ref. 11.

For the supernova events, after the vertex position of an event is found, a good approximate energy is given by the number of hit PMT, $N_{\rm hit}$, for which the residual time (t_i − time of flight from vertex to PMT$_i$) is within ±15 nsec, where t_i is the measured time in PMT$_i$. The single photoelectron time response of the PMT is 13 nsec full width at half maximum (FWHM). For Monte Carlo events generated throughout the detector using the energy scale discussed in Ref. 11, $N_{\rm hit}=26$ corresponds to 10 MeV total energy and $N_{\rm hit}=73$ corresponds to 30 MeV. There is no significant difference between the energy scales for electrons and positrons in the detector. The calorimetric response of the detector compensates for the slight differences in energy-loss mechanisms between electrons and positrons.

For each supernova-induced event, the actual energy determination utilized the reconstructed event vertex. Sets of Monte Carlo events of fixed energy differing by a small amount from that inferred from the scale in the preceding paragraph were generated with the vertices in each set varied within the vertex resolution described above. The generated angles were not varied since the multiple scattering, which is included in the Monte Carlo calculation, dominates the angular resolution. The $N_{\rm hit}$ distributions of each Monte Carlo event set were compared to the $N_{\rm hit}$ of the actual event. The estimated energy for the event was chosen to be that energy for which the mean $N_{\rm hit}$ of the Monte Carlo data reproduced the $N_{\rm hit}$ of the event.

C. Trigger rate

At the time that the neutrino burst from SN1987A was observed, the total rate of triggers in the detector was 0.60 Hz on average, of which 0.37 Hz was due to penetrating cosmic-ray muons. The total trigger rate had been stable at that value for several months, apart from small perturbations introduced by efforts to reduce the amount of ^{222}Rn (half-life 3.8 days) dissolved in the tank water. At the low-energy trigger rate of 0.23 Hz, most of the rate is due to the β decay of ^{214}Bi (β spectrum end point 3.26 MeV), a daughter of ^{222}Rn. A smaller fraction of the 0.23-Hz rate comes from γ rays and neutrons from radioactive elements in the walls of the mine cavity and the detector itself, e.g., the PMT. The presence of ^{222}Rn which is dissolved in the water is observed by measuring its lifetime when fresh water is added to the main detector; the detection of low energy of electrons from the ^{214}Bi decay results from the energy resolution and trigger time window of the detector for few MeV electrons, and is done with an efficiency $\lesssim 10^{-4}$.

III. THE NEUTRINO BURST

Scatter plots of $N_{\rm hit}$ against time during a number of 17-min intervals on 23 February 1987 are given in Fig. 4. In these plots each point represents a single event with a given value of $N_{\rm hit}$ which occurred at the time indicated. Most of the observed events have $N_{\rm hit} \leq 20$; the average rate of events with $N_{\rm hit} > 23$ during the 10-h period from 2:27 UT to 22:27 UT is $\leq 10^{-2}$ Hz. The events with $N_{\rm hit} \leq 20$ are largely due to ^{214}Bi decay, while those with $N_{\rm hit} \geq 23$ are consistent with higher-energy products of radioactivity at or outside the tank wall. We have also let stand in Fig. 4 a number of events known to have been produced by muon interactions in the detector water (see below) to convey the nature of the data in its almost raw state. A scatter plot of the radial (r) and longitudinal (z axis of the detector) distribution of the vertices of events in the 10-h interval with $N_{\rm hit} \geq 23$, shown in Fig. 5(a), makes clear the concentration of such events at the surface of the detector. The scatter plots of z and r versus cosine of the angle with respect to the normal to the surface of the nearest PMT, shown in Figs. 5(b) and 5(c), show the direction of those events to be inward to the central volume of the detector.

The neutrino burst at 7:35:35 UT is evident in Fig. 4(e). The coordinates and direction cosines of the electrons or positrons of the 12 events in the 13-sec time interval beginning at 7:35:35 UT, relative to x, y, and z axes with origin at the center of the detector, are given in Table I. The occurrence times, energies, and angles relative to the LMC are given in Table II. Since the burst data were presented in Ref. 6, an independent program has been used to check on the reconstruction of the 12 events in the burst. Within the known error in reconstruction, the coordinates of the vertex positions of all events obtained from the two programs are in excellent agreement. In addition, there is agreement between the results of the two programs on the energies of all events within the quoted error.[6] Furthermore, with one exception, all of the reconstructed angles with respect to the LMC from the two programs agree within one standard deviation. The sole exception occurs in event 2 for which the original reconstruction gave $\theta(e,\text{LMC}) = (15\pm27)$ deg, while the later reconstruction yields $\theta(e,\text{LMC}) = (40\pm27)$ deg. This

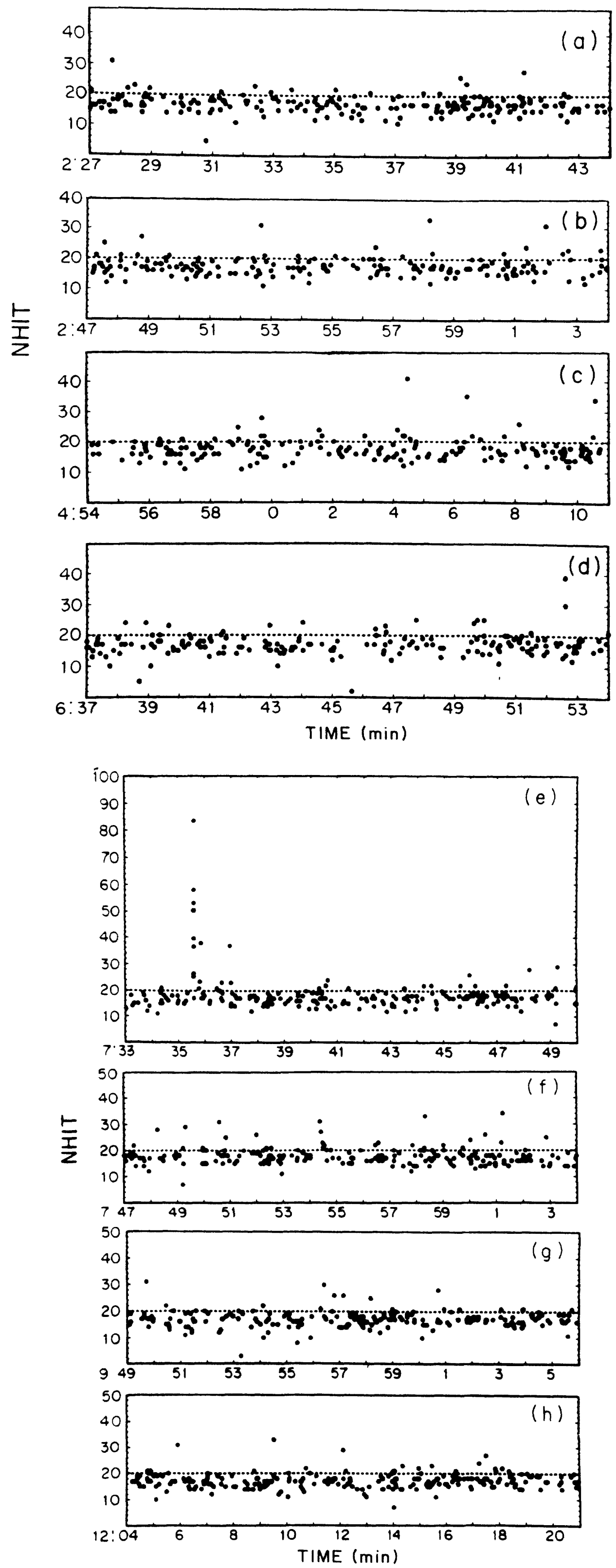

FIG. 4. Scatter plots of $N_{\rm hit}$ against time for eight intervals of 17-min duration in the time period covering 5 h before and 5 h after the neutrino burst at 7:35:35 UT. Six of the eight intervals were chosen at random. The interval beginning at 2:47 UT contains the time (2:52 UT) at which an event burst was reported by M. Aglietta *et al.* [Europhys. Lett. **3**, 1315 (1987)].

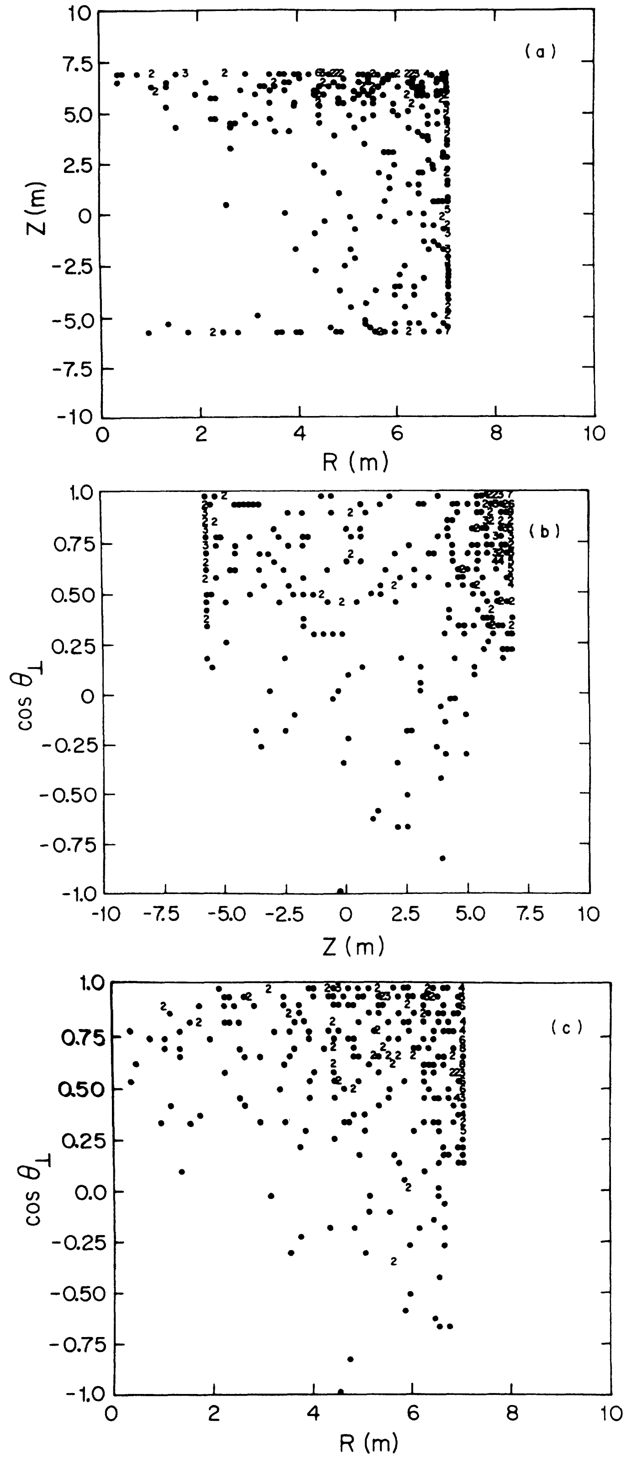

FIG. 5. (a) Scatter plot of the radial (r) and longitudinal (z) coordinates of the 355 events with $N_{\rm hit} \geq 23$ in the 10-h time period discussed in the text. (b) Scatter plot of longitudinal (z) coordinates and direction cosines with respect to the normal to the surface of the nearest PMT of the events in (a). (c) Scatter plot of the radial (r) coordinates and direction cosines with respect to the normal to the surface of the nearest PMT of the events in (a). The origin of the z axis is 0.60 m below the geometric center of the tank. Low-energy events with vertices within 1 m of an edge of the fiducial volume are reconstructed to a common position 0.25 m from that edge by the reconstruction program.

result lessens the likelihood that event 2 originated from ν_e scattering; otherwise the event reconstructions and interpretation given in Ref. 6 remain unchanged. The observed patterns of hit PMT for events 1, 9, and 12 are shown as examples of such events in Figs. 6–8.

A plot showing all events, including through-going muons, observed in an interval of 48 sec surrounding 7:35:35 UT is given in Fig. 9. We have considered the possibility that the event burst at 7:35:35 UT might have been caused by one or more of the muons in Fig. 9. This possibility may be unequivocally rejected as follows. The characteristics of events produced in energetic nuclear cascades by cosmic-ray muons have been studied in detail for the energy calibration, and as a spallation background for solar-^{8}B neutrino events.[11] The relative rate of spallation leading to one or more low-energy electron events is less than 10^{-3} per incident muon. The measured multiplicity distribution of low-energy electron events following an incident muon in time yields a probability of multiplicity ≥ 3 of 3×10^{-3}. The low-energy electron-event background from spallation has the following principal properties: (1) It consists of a component which exhibits an exponential time structure with half-life 18.2 ± 1.8 msec, and also a component with a longer exponential time structure of 1.2 ± 0.5 sec, with relative rates 2:1, respectively; and (2) the resultant β-decay electrons with observed energies above 15 MeV occur with less than 4% probability.

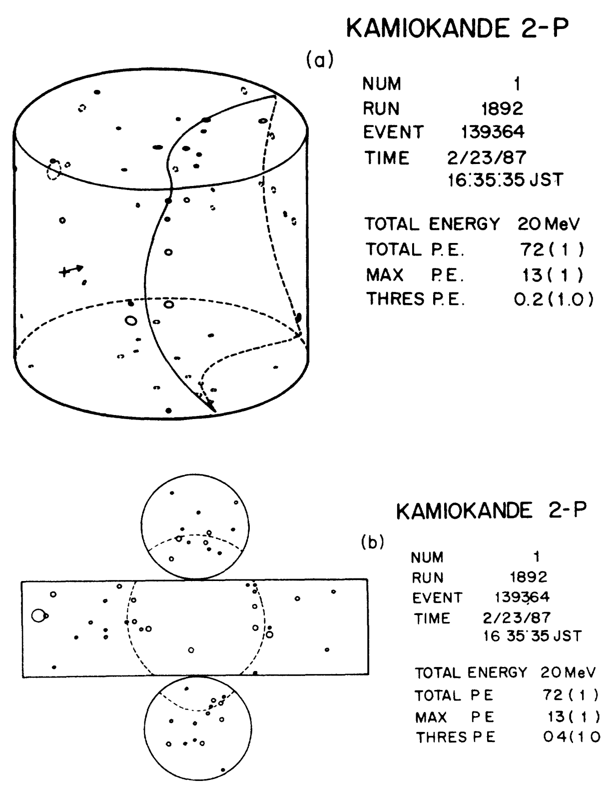

FIG. 6. (a) Three-dimensional reproduction of event 1 listed in Tables I and II. (b) Exploded view of event 1. Each small circle represents a struck PMT; the diameter of the circle is proportional to the charge output of the PMT. The numbers in parentheses refer to quantities measured in the anticounter.

TABLE I. Cartesian coordinates and directional cosines with respect to axes in the detector of the 12 observed SN1987A neutrino-induced events. The system of axes is right handed with the z axis along the detector zenith.

Event	x	y	z	$\cos\alpha$	$\cos\beta$	$\cos\gamma$
1	2.64	−4.43	−1.88	−0.441	0.867	0.234
2	−1.09	−7.03	3.26	−0.841	0.049	0.539
3	−6.72	2.29	−5.51	0.838	0.078	0.542
4	3.75	6.13	−5.63	−0.793	−0.460	0.399
5	−2.00	5.03	6.47	−0.073	−0.909	−0.409
6	−3.87	0.13	−4.00	−0.325	0.606	−0.726
7	3.69	−5.35	−5.82	−0.812	0.189	0.553
8	4.51	−5.57	−2.98	−0.481	0.427	0.766
9	2.08	0.41	1.50	−0.806	0.087	0.585
10	−5.56	−4.54	7.01	0.641	0.211	0.737
11	3.65	−2.16	−1.73	−0.191	0.334	0.923
12	0.83	−4.21	−0.97	0.281	−0.221	0.934

Consequently, the overall probability that any of the muons, $\mu 1$ to $\mu 4$, was the progenitor of the event burst in Table II is extremely low, much less than $10^{-3}\times 3\times 10^{-3}\times(0.04)^4$, where the last factor follows from taking the four events (Nos. 1, 7, 8, and 9) in Table II with $(E_e-1\sigma)>15$ MeV. Note that the probability of 8×10^{-12} does not include factors from either the details of the internal time structure of the data in Table II, or the time separation of the entire burst from any of the preceding muons, or the geometrical correlation of the low-energy electrons from spallation with the muons that produced them.

We have also searched the data over a period of 2.7 days from 21 February to 24 February to determine the statistical significance of the burst at 7:35:35. This is indicated by the Poisson distributions shown in Fig. 10 for events with $N_{\rm hit}\geq 20$ and $N_{\rm hit}\geq 30$. It is seen that the probability of occurrence of a burst with 9 events per 10 sec ($N_{\rm hit}\geq 20$) or 6 events per 10 sec ($N_{\rm hit}>30$), based on the observed distributions in Fig. 10, is less than 5.7×10^{-8} or less than 1.4×10^{-8}, respectively, for the 2.7-day interval. In addition, a search was made on a larger data sample of 42.9 days, 9 January 1987 to 25 February 1987, and no other burst candidates were found, where a burst candidate was defined as an event multiplicity ≥ 4 per 10 sec with $N_{\rm hit}$ per event ≥ 30.

Furthermore, we have intensively searched the data in the 10-h period from 2:27 UT to 12:27 UT for any evidence of other event bursts, perhaps smaller in event number or lower in energy than the burst at 7:35:35 UT. For events with $N_{\rm hit}>20$ in that period there is no event cluster per 10-sec interval that deviates from the Poisson distribution in Fig. 10(a). It has also been shown in Fig. 5 that the r-z, $z-\cos\theta_\perp$, and $r-\cos\theta_\perp$ distributions of events with $N_{\rm hit}>23$ are consistent with events mainly emanating from the detector surfaces and not a volume distribution. In addition, we show in Fig. 11 histograms of the numbers of events per 30 sec with $N_{\rm hit}\leq 20$ in eight 17-min periods corresponding to those in Fig. 4. There is no evidence of any statistically significant excess of events

TABLE II. Measured properties of the 12 electron events detected in the SN1987A neutrino burst. The angle in the last column is relative to the direction of the LMC. The errors on electron energies and angles are one-standard-deviation Gaussian errors.

Event number	Event time (sec)	Number of PMT ($N_{\rm hit}$)	Electron energy (MeV)	Electron angle (deg)
1	0	58	20.0±2.9	18±18
2[a]	0.107	36	13.5±3.2	40±27
3	0.303	25	7.5±2.0	108±32
4	0.324	26	9.2±2.7	70±30
5	0.507	39	12.8±2.9	135±23
6	0.686	16	6.3±1.7	68±77
7	1.541	83	35.4±8.0	32±16
8	1.728	54	21.0±4.2	30±18
9	1.915	51	19.8±3.2	38±22
10	9.219	21	8.6±2.7	122±30
11	10.433	37	13.0±2.6	49±26
12	12.439	24	8.9±1.9	91±39

[a]See text.

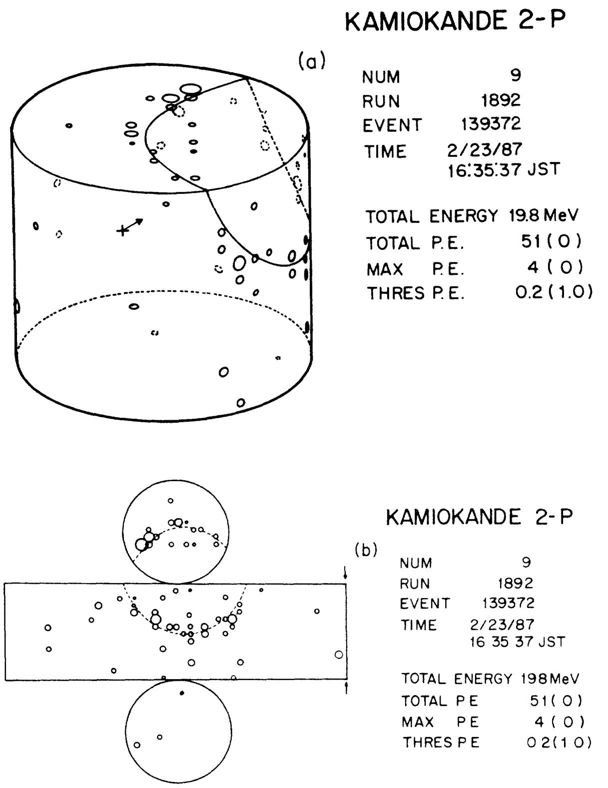

FIG. 7. (a) Three-dimensional reproduction of event 9 listed in Tables I and II. (b) Exploded view of event 9.

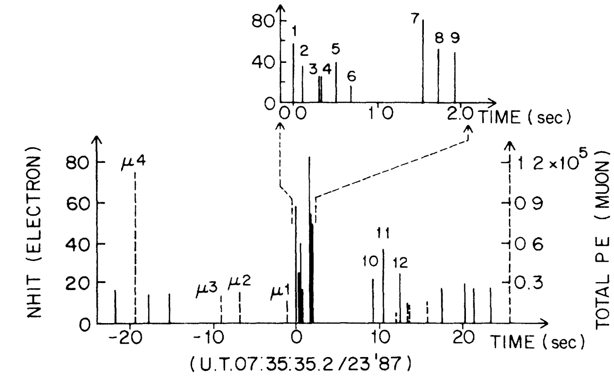

FIG. 9. The time sequence of events in a 45-sec interval centered on 7:35:35 UT 23 February 1987. The vertical height of each line represents the relative energy of the event. Solid lines represent low-energy electron events in units of the number of hit PMT, N_{hit} (left-hand scale). Dashed lines represent muon events in units of the number of photoelectrons (right-hand scale). Events $\mu 1$–$\mu 4$ are muon events which precede the electron burst at time zero. The upper right figure is the 0–2-sec time interval on an expanded scale.

with $N_{hit} \leq 20$ in any of those 17-min periods. The Poisson distribution for events with $N_{hit} \leq 20$ per 30 sec for the entire 10-h period 2:27 UT to 12:27 UT is shown in Fig. 12, and indicates that an excess of 10 events above the mean of 5.4 events in a 30-sec interval would be recognized. This result holds proportionally if the unit of time is chosen to be 10 sec rather than 30 sec.

Finally, a sample of triggers was chosen primarily to monitor the trigger rate, for which the trigger threshold was lowered to $N_{hit} \approx 14$, corresponding to 5.6 MeV at which energy the efficiency was roughly 35%. During the 12.44-sec interval of the observed neutrino burst (Table II), the observed number of triggers (after subtracting the supernova burst) was 138±12, compared with the expected value of 127 obtained from the average background trigger rate of 10.2 Hz for several subruns around the supernova time. During the 10-sec interval between 2:52:36 UT and 2:52:46 UT, there were 99±10 triggers when 102 were expected from nearby time intervals.

We conclude that there is no evidence in the data of Kamiokande-II for any excess of neutrino-induced events—either in a burst of a few seconds or over a longer time interval—relative to the usual count rate, excepting only the neutrino burst at 7:35:35 UT.

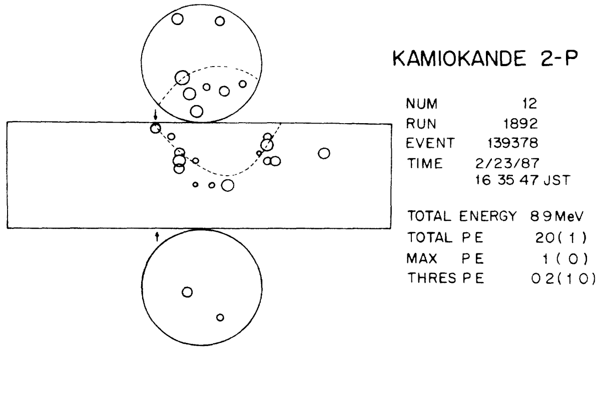

FIG. 8. Exploded view of event 12.

IV. ANALYSIS AND INTERPRETATION OF THE BURST DATA

The total energy and angle relative to the LMC of the 12 electrons observed in the burst are given in two columns of Table II. For each event the energy and the 1σ error on the energy were calculated as described in Sec. II B. The approximately Gaussian errors on $\theta(e,\text{LMC})$ in Table II were obtained from the Monte Carlo events used to estimate the event energies and uncertainties.

A scatter plot of E_e vs $\cos\theta(e,\text{LMC})$ is shown in Fig. 13(a), and projections on each axis in Figs. 13(b) and 13(c). The angular distribution in Fig. 13(c) is consistent with an isotropic distribution of the electrons relative to LMC. This is in turn consistent with the energy dependence of the neutrino cross sections[12] shown in Fig. 14(a), where it is seen that the dominant cross section is $\sigma(\bar{\nu}_e p_{\text{free}} \to e^+ n)$ with the isotropic angular distribution given in Fig. 14(b). Accordingly, the energy of the incident $\bar{\nu}_e$ is given by $E(\bar{\nu}_e) = E(e^+) + (m_n - m_p)$

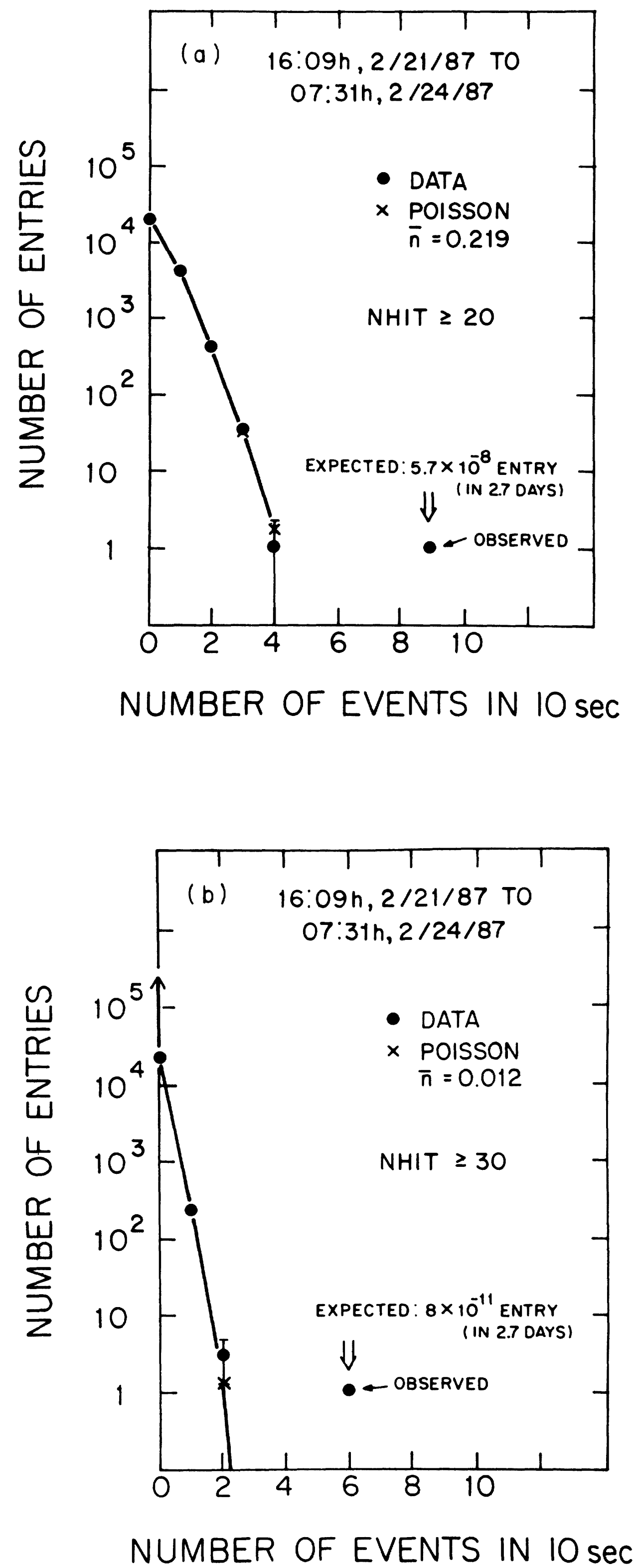

FIG. 10. (a) Poisson distribution of the number of events with $N_{\rm hit} \geq 20$ per 10 sec in a 2.7-day period surrounding the time 7:35:35 UT. (b) Poisson distribution of the number of events with $N_{\rm hit} \geq 30$ per 10 sec in a 2.7-day period surrounding the time 7:35:35 UT.

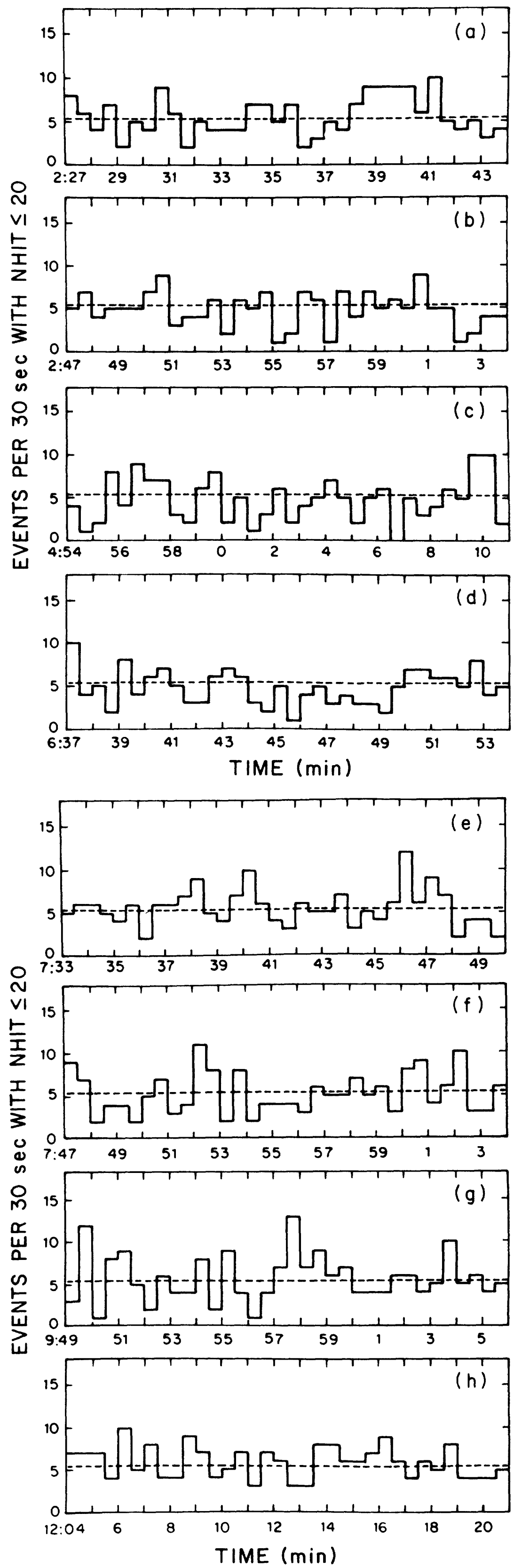

FIG. 11. Histograms of the number of events per 30 sec with $N_{\rm hit} \leq 20$ as a function of time for the same eight intervals as in Fig. 4. The horizontal dashed lines indicate the mean value of the Poisson distribution in Fig. 12.

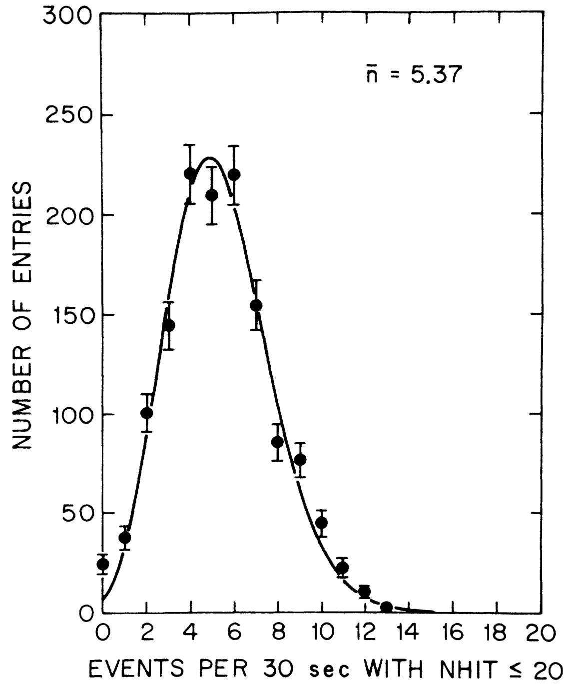

FIG. 12. Poisson distribution of the number of events per 30 sec with $N_{\text{hit}} \le 20$ in the 10-h period surrounding the time 7:35:35 UT.

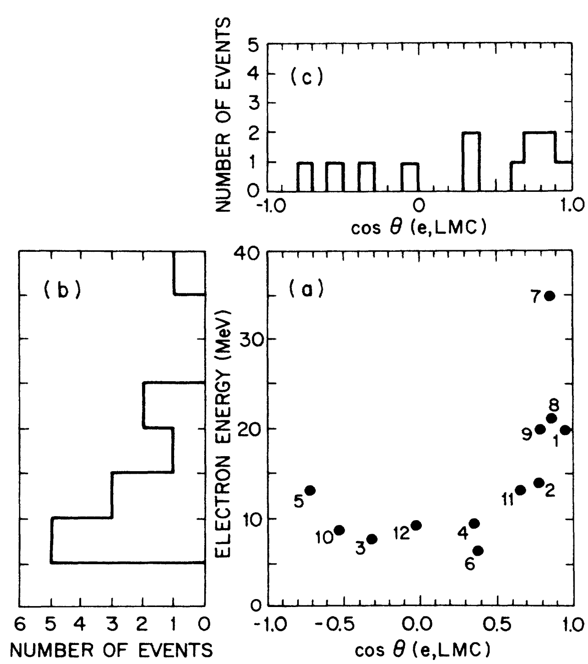

FIG. 13. (a) Scatter plot of the detected electron energy (in MeV) and the cosine of the angle between the measured electron direction and the direction of the Large Magellanic Cloud. The number to the left of each entry is the time-sequential event number from Tables I and II. The two projections of the scatter plot are displayed in (b) and (c).

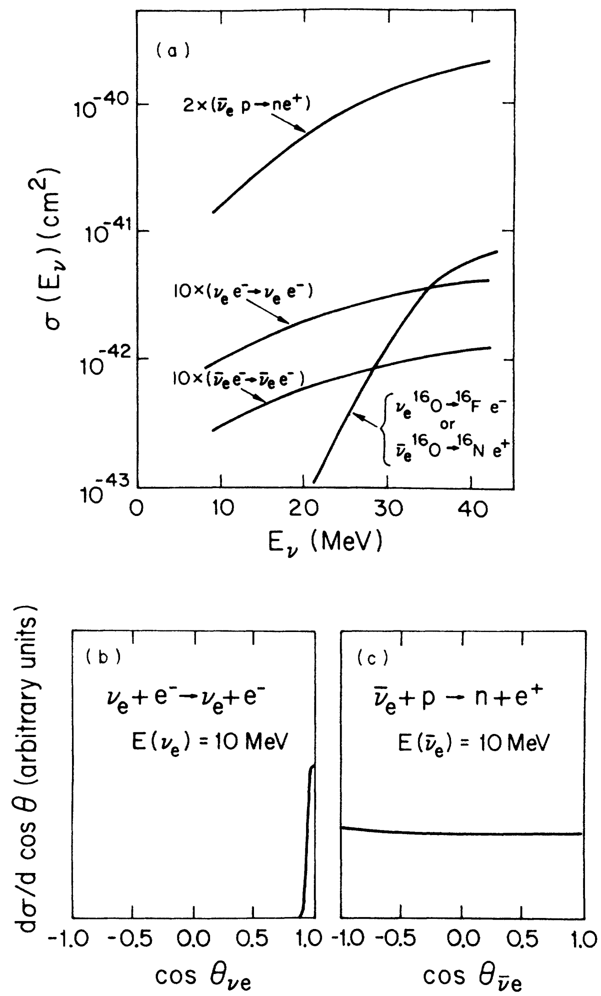

FIG. 14. (a) Plot of $\sigma(E_\nu)$ vs E_ν for several $\nu(\bar{\nu})$ reactions. (b) Plot of $d\sigma/d\cos\theta_{\nu e}$ for the reactions $\nu_e e \to \nu_e e$ and $\bar{\nu}_e p \to e^+ n$.

$=E(e^+) + 1.3$ MeV, and is so calculated for all but the first event in the burst. Event 1 is consistent with production through $\sigma(\nu_e e^- \to \nu_e e^-)$. [The latter reconstruction program yielded for event 1, $\theta(e,\text{LMC}) = (10\pm 18)$ deg in agreement with the original value of (18 ± 18) deg.] As seen from Fig. 14, of order one event from that reaction might be expected in Kamiokande-II.

Given the electron energies in Table II, the electron detection efficiency versus energy relationship in Fig. 3, and assuming all but event 1 are due to $\bar{\nu}_e p_{\text{free}} \to e^+ n$, the resultant integrated flux of $\bar{\nu}_e$ in the burst at 7:35:35 is 1.1×10^{10} cm^{-2} for $\bar{\nu}_e$ with energies above 8.8 MeV. This in turn leads to a $\bar{\nu}_e$ output of SN1987A of 9×10^{52} ergs for an (observed) average energy of 15 MeV.

The internal time structure and the energies of the events in the burst, as given in Fig. 9 and Table II, have been addressed in studies[13] that attempt to extract the initial-state properties and time evolution of SN1987A. A detailed, precise comparison of the burst data from Kamiokande-II and from the IMB detector[9] is not possible because the absolute time of the beginning of the neutrino burst in Kamiokande-II is given with an error of ± 1

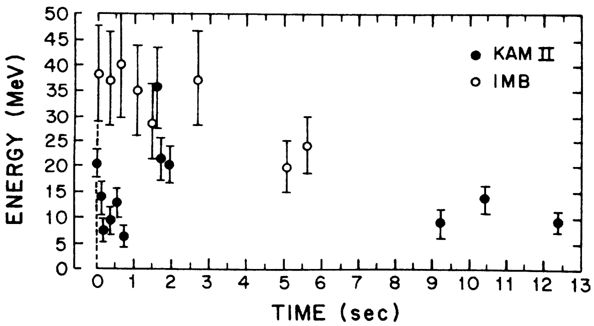

FIG. 15. Scatter plot of energy and time of the 12 events in the burst sample observed in Kamiokande-II, and the 8 events in the burst sample observed in the IMB detector. The earliest event in the sample of each detector has, arbitrarily but not unreasonably, been assigned $t=0$.

min, the uncertainty arising from the absence of an absolute time calibration source in the Kamiokande-II equipment. It would have been straightforward after SN1987A to have made an absolute calibration of the clock in the event time circuit (see Fig. 2) which assigned a precise relative time to each event, but an abrupt power outage took place in the Kamioka mine on 25 February 1987, and precluded that alternative measure. If it is assumed, arbitrarily but not unreasonably, that the earliest events observed by the two detectors coincided in time, the plot in Fig. 15 is obtained. Figure 15 suggests that the two observations agree on a cluster of 14 events within the first 2 sec, and indicates a tailing off of the remaining 6 events to 12.44 sec.

V. SUMMARY AND CONCLUSIONS

The event burst at 7:35:35 UT, 23 February 1987, observed in Kamiokande-II, is a genuine neutrino burst. This is the only burst found in Kamiokande-II during the period 9 January to 25 February 1987. Intensive analyses of the Kamiokande-II data of shorter time intervals surrounding 7:35:35 UT have yielded no statistically significant evidence for another similar burst of perhaps fewer events, or of an enhanced rate in the lower-energy region of the background in the detector. We conclude, therefore that the burst on 23 February 1987 at 7:35:35 UT was the only burst observed in Kamiokande-II.

The properties of the event burst coincide remarkably well with the current model of the basic nature of type-II supernovae and neutron-star formation. The observed energies of the neutrinos, their number, and type of interaction, in conjunction with the time duration of the burst, are consistent with the free-fall collapse of the core of a massive star, and the evaporation within a few seconds of all flavors of neutrino-antineutrino pairs with total energy amounting to $\sim 3\times 10^{53}$ ergs from the newly born neutron star at temperature $kT \approx 4$ MeV. To elicit descriptions and explanations of more specific properties such as, for example, the time separation of events within the burst, the time interval between the core collapse, and the earliest optical sighting, and the possible influence of the bounce of the in-falling massive core and the resultant shock wave on neutrino emission is the subject of much present theoretical study.

There are two principal conclusions of significance in elementary-particle physics which may be reached from the Kamiokande-II neutrino burst data. First, the lifetime of ν_e and $\bar{\nu}_e$ must be greater than about $1.7\times 10^5[m(\nu_e)/E(\nu_e)]$ yr, taking the distance to the LMC to be 55 kpc. Second, an upper limit on the mass of ν_e and $\bar{\nu}_e$ may be obtained from the burst data subject to simplifying assumptions. The totality of attempts to do so using a variety of assumptions has led to upper-limit estimates ranging[14] from a few eV to 24 eV.

The observation in Kamiokande-II and in the IMB detector of the neutrino burst from SN1987A is the first direct observation in neutrino astronomy. The coincidence in time with the optical sighting of SN1987A, and the clarity of the burst signal in the neutrino detectors suggest that future observations in neutrino astronomy may well proceed independently of other astronomical observations. If the expected rate of occurrence of supernovae in the Galaxy,[15] i.e., one supernova per 10–20 yr, is roughly correct, the detailed study of neutron-star, and perhaps even black-hole, formation may become a reality, providing that adequate neutrino telescopes are maintained as active instruments over long periods of time. Clearly, observation of additional neutrino bursts from supernovae would also contribute importantly to improved determinations of the intrinsic properties of neutrinos.

ACKNOWLEDGMENTS

We gratefully acknowledge the cooperation of the Kamioka Mining and Smelting Co. This work was supported by the Japanese Ministry of Education, Science and Culture, the United States Department of Energy, and the University of Pennsylvania Research Fund.

*Present address: AT&T Bell Laboratories, Holmdel, New Jersey.

[1]See, for example, Paul Murdin and Lesley Murdin, *Supernovae*, revised edition (Cambridge University Press, Cambridge, 1985); and D. H. Clark and F. R. Stephenson, *The Historical Supernovae* (Pergamon, Oxford, 1977).

[2]F. Zwicky, in *Stellar Structure*, edtied by G. P. Kuiper and B. M. Middlehurst (University of Chicago Press, Chicago, 1965).

[3]S. Chandrasekhar, Astrophys. J. **24**, 81 (1931).

[4]H. Y. Chiu, Ann. Phys. (N.Y.) **26**, 364 (1964); S. A. Colgate and R. H. White, Astrophys. J. **143**, 626 (1966); S. E. Woosley, James R. Wilson, and Ron Mayle, *ibid*. **302**, 19 (1986).

[5]W. Baade and F. Zwicky, Proc. Natl. Acad. Sci. U.S.A. **20**, 254 (1934); W. A. Fowler and F. Hoyle, Astrophys. J. Suppl. **9**, 201 (1964); S. A. Colgate and R. H. White, Astrophys. J. **143**, 626 (1966); W. D. Arnett, Annu. Rev. Astron. Astrophys. **11**, 73 (1973); H. A. Bethe *et al.*, Nucl. Phys. **A324**, 487 (1979); R. L. Bowers and J. R. Wilson, Astrophys. J. Suppl. **50**, 115 (1982); W. D. Arnett, Astrophys. J. **263**, L55 (1983); H. B. Bethe and J. R. Wilson, *ibid*. **295**, 14 (1985); A. Burrows and

J. M. Lattimer, *ibid.* **307**, 178 (1985); J. R. Wilson *et al.*, Ann. N.Y. Acad. Sci. **470**, 267 (1986); E. S. Myra *et al.*, Astrophys. J. **318**, 744 (1987).

[6]K. Hirata *et al.*, Phys. Rev. Lett. **58**, 1490 (1987).

[7]R. P. Kirschner *et al.*, Astrophys. J. **320**, 602 (1987); N. R. Walburn *et al.*, *ibid.* **321**, L41 (1987).

[8]I. Shelton, IAU Circular No. 4316 (unpublished). Note also that R. H. McNaught subsequently communicated visual magnitude of 6.0 on February 23.443 UT, *ibid.*

[9]R. M. Bionta *et al.*, Phys. Rev. Lett. **58**, 1494 (1987).

[10]K. Arisaka, Ph.D. thesis, Tokyo University, Report No. UT-ICEPP-85-01, 1985; T. Kajita, Ph.D. thesis, Tokyo University, Report No. UT-ICEPP-86-03, 1986. See also M. Nakahata, J. Phys. Soc. Jpn. **55**, 3786 (1986).

[11]K. Hirata *et al.*, in *The Standard Model: Supernova 1987A*, proceedings of the XXIInd Rencontre de Moriond, Les Arcs, France, 1987, edited by J. Tran Thanh Van (Editions Frontières, Gif-sur-Yvette, 1987), p. 689; (unpublished); M. Nakahata, Ph.D. thesis, Tokyo University, 1987.

[12]U. Amaldi *et al.*, Phys. Rev. D **36**, 1385 (1987).

[13]See, for example, J. N. Bahcall *et al.*, Nature (London) **327**, 682 (1987); Kolb, Stebbins, and Turner (Ref. 14); Abbott, De Rújula, and Walker (Ref. 14); Burrows (Ref. 14); Sidney A. Bludman and Paul J. Schnider, Astrophys. J. **326**, 265 (1988).

[14]The following comprise references which are directly identified. Published papers are given first, and reports are listed in alphabetical order of the first author's name: J. N. Bahcall and S. L. Glashow, Nature (London) **326**, 476 (1987); W. D. Arnett and J. L. Rosner, Phys. Rev. Lett. **58**, 1906 (1987); K. Sato and H. Suzuki, *ibid.* **58**, 2722 (1987); J. Arafune and M. Fukugita, *ibid.* **59**, 367 (1987); E. W. Kolb, A. J. Stebbins, and M. S. Turner, Phys. Rev. D **35**, 3598 (1987); **36**, 3820 (1987); S. H. Khara, J. Cooperstein, and E. Baron, Phys. Lett. B **196**, 359 (1987); A. Burrows and J. M. Lattimer, Astrophys. J. Lett. **318**, L63 (1987); I. Goldman *et al.*, Phys. Rev. Lett. **60**, 1789 (1988); K. Hikasa, M. Kobayashi, and M. Yoshimura, Prog. Theor. Phys. **78**, 180 (1987); S. Midorikawa, H. Terazawa, and K. Akama, Mod. Phys. Lett. **A2**, 561 (1987); M. Roos, in *The Standard Model: Supernova 1987A* (Ref. 11), p. 761; L. F. Abbott, A. De Rújula, and T. P. Walker, Nucl. Phys. **B299**, 734 (1988); A. Burrows, Arizona Theoretical Astrophysics Report No. 87-12, 1987 (unpublished); Z. M. Chen *et al.*, Beijing Institute for Theoretical Physics Report No. BIHEP TH-875, 1987 (unpublished); C. R. Ching, T. H. Ho, Z. J. Tao, and Z. X. Huo, Academia Sinica Report No. ITP-87-015, 1987 (unpublished); H. Y. Chiu, Y. Kondo, and L. L. Chan, GSFC Report, 1987 (unpublished); J. A. Cowen and W. W. Repko, Michigan State University report, 1987 (unpublished); R. Cowsik, Washington University report, 1987 (unpublished); A. Dar and S. Dado, Technion Report No. TECH-PH-0000, 1987 (unpublished); D. Evans, R. Fong, and P. D. B. Collins, Durham University Report No. DTP/87/12, 1987 (unpublished); J. Franklin, Temple University Report No. HE-87-52, 1987 (unpublished); C. W. Kim and W. K. Sze, Report No. JHU-HEP-8705, 1987 (unpublished); L. M. Krauss, Report No. YTP 87-16, 1987 (unpublished); M. Roos, Helsinki University Report No. HU-TFT-87-25, 1987 (unpublished); R. E. Schrock, SUNY Report No. ITP-SB-87-18, 1987 (unpublished); J. J. Simpson, Guelph University Report No. (GWP)-NP-10, 1987 (unpublished); D. N. Spergel and J. N. Bahcall, Institute for Advanced Study report 1987 (unpublished); J. Thierry-Mieg, Cambridge University Report No. 87-0236, 1987 (unpublished); C. M. Xu, X. J. Wu, and T. P. Li, Beijing Institute of Theoretical Physics report, 1987 (unpublished).

[15]J. N. Bahcall and T. Piran, Astrophys. J. **267**, L77 (1983).